

This article was downloaded by:

On: 16 April 2009

Access details: *Access Details: Free Access*

Publisher *Taylor & Francis*

Informa Ltd Registered in England and Wales Registered Number: 1072954 Registered office: Mortimer House, 37-41 Mortimer Street, London W1T 3JH, UK



## Aerosol Science and Technology

Publication details, including instructions for authors and subscription information:

<http://www.informaworld.com/smpp/title-content=t713656376>

### A Partial Theory of Atomization in Internal Mix Swirl Nozzles

David E. Dietrich<sup>a</sup>

<sup>a</sup> Edodynamics Research Associates, Albuquerque, NM

First Published on: 01 January 1990

**To cite this Article** Dietrich, David E.(1990)'A Partial Theory of Atomization in Internal Mix Swirl Nozzles',*Aerosol Science and Technology*,12:3,654 — 664

**To link to this Article:** DOI: 10.1080/02786829008959380

**URL:** <http://dx.doi.org/10.1080/02786829008959380>

PLEASE SCROLL DOWN FOR ARTICLE

Full terms and conditions of use: <http://www.informaworld.com/terms-and-conditions-of-access.pdf>

This article may be used for research, teaching and private study purposes. Any substantial or systematic reproduction, re-distribution, re-selling, loan or sub-licensing, systematic supply or distribution in any form to anyone is expressly forbidden.

The publisher does not give any warranty express or implied or make any representation that the contents will be complete or accurate or up to date. The accuracy of any instructions, formulae and drug doses should be independently verified with primary sources. The publisher shall not be liable for any loss, actions, claims, proceedings, demand or costs or damages whatsoever or howsoever caused arising directly or indirectly in connection with or arising out of the use of this material.

---

# A Partial Theory of Atomization in Internal Mix Swirl Nozzles

David E. Dietrich

*Ecodynamics Research Associates, P.O. Box 8172, Albuquerque, NM 87198*

---

A partial theoretical description of mixing and atomization processes in an opposed swirl nozzle is presented. Explanations based on fluid instability and nonlinear mixed-layer effects are offered for several observations: although volume mean drop size is re-

lated to sheet thickness in swirl atomizers, these produce a large range of drop sizes; ligament formation occurs before separation and drop formation; and slurry atomization performance is often similar to atomization of the liquid carrier without slurry particles.

---

## 1. INTRODUCTION

The dynamics of drop formation or "atomization," and related mixing processes in nozzles, is an intriguing subject rich in fluid dynamic phenomena that are not understood in detail. However, a partial theoretical description of mixing and atomization can be derived from known fluid behavior.

The simplest nozzles direct the bulk liquid at high velocity into a passive external gas. The resulting spray has rather high velocity in the direction of the original bulk liquid motion. Although useful for some applications, this does not efficiently apply the original bulk liquid energy to atomization dynamics. For processes in which the primary goal is to produce small drops, this wastes energy.

Such energy waste can be reduced by directing pressurized gas in a direction opposite to the liquid. The resulting liquid-gas shear is very large, and the bulk liquid and gas momentum can be greatly reduced by mutual interaction during atomization. Such opposed flow nozzles are most efficient when complete mixing occurs inside the nozzle, greatly reducing the opposed flow energy internally, rather than allowing this energy to be needlessly wasted in mixing with a passive environment outside the nozzle.

Thus, internal mix nozzles are of great interest. A review of various types of nozzles is given by Simmons (1979).

Internal mix nozzles using opposed swirl have several advantages (Dietrich, 1982, 1985). Perhaps their greatest advantages are that they confine the injected fluids until they are thoroughly mixed, and provide very effective mechanisms by which to achieve such mixing. Thus, internal mix opposed swirl nozzles are of special interest.

In Section 2, we discuss fluid mechanisms relating to nozzles in general. In Section 3, we apply these mechanisms to develop a partial theory on mixing and atomization in opposed swirl nozzles.

## 2. GENERAL THEORY

First, we briefly discuss some important concepts. We will use the term basic flow to denote the time averaged flow. The basic flow is most meaningful under steady operating conditions (under constant external pressure conditions for a nozzle with fixed internal boundaries). However, it is also a useful concept when they are time dependent, especially when they are relatively steady during a typical fluid residence time.

Even with exactly steady operating conditions, turbulent fluctuations occur which are deviations from the basic flow. The fluctuations occur due to fluid instabilities associated with the basic flow structure. The fluctuations are associated with transient small-scale eddies. These turbulent eddies accomplish the fluid deformations required by mixing and atomization processes. Thus, the space-scales and intensities of these eddies determine nozzle performance.

It follows that nozzle performance is determined by the basic flow distribution imposed by its inflow conditions and internal structure. The basic flow distribution determines fluid instability and associated turbulence distribution. Conversely, the basic flow is itself affected by the turbulence in a very nonlinear manner, including important shears and recirculation zones. While the basic flow is not necessarily an appropriate base state for stability analysis, it can suggest appropriate base states for such analysis.

In summary, atomization involves fluid instabilities in a very nonlinear basic flow. These instabilities result in the growth of small-scale eddies, which accomplish the mixing deformations leading to drop separation from the bulk liquid. Efficient atomization is promoted by forcing a basic flow pattern in which the flow near the interface between the bulk liquid and gas is unstable to eddies whose axis (or vorticity vector) lies approximately in the plane of the interface.

Sometimes the bulk liquid to be atomized contains a dense solid particle suspension (such as in slurries). It has been noted (Simmons, 1984; Gaag, 1984) that such slurry atomization is sometimes not strongly inhibited by the presence of solid particles and can be quite similar to the atomization of the liquid phase alone under similar operating conditions with the same nozzle.

A possible interpretation of this is that atomization is a discontinuous process, analogous to the fracturing of solids, involving fluid properties in only a secondary manner.

However, atomization processes are very fast and therefore can appear discontinuous, even when governed by continuum fluid properties. Observations might resolve only the relatively slow final breakup, when drops separate from the bulk liquid, and miss much more rapid processes upstream, where fluid instabilities lead to small-scale turbulent eddies which deform the bulk liquid surface and determine drop size. Indeed, early calculations from an opposed swirl model (Dietrich, 1987) reveal a mechanism for "microburst" behavior in which drops are continually separated from the bulk liquid sheet by intense, short-lived jets of gas that penetrate through the liquid sheet toward the nozzle centerline. Such instabilities convert the bulk flow kinetic energy to small-scale eddy energy that does work against surface tension and viscous forces. Some of the increased surface energy is released during the final breakup.

Observations combined with a simple theory (see Appendix A) indicate that continuum fluid properties involving pressure and viscous forces dominate before the final breakup. Energy balance considerations show that if drop size is inversely proportional to the square root of the pressure drop for a given nozzle and operating fluid, viscous forces are probably more important than surface tension forces in determining drop size in the range of operating conditions covered by the data. This inverse square root relation dominates observations in the literature (Jasuja, 1978; Dietrich, 1982; Elkotb and Abdalla, 1982; Jones, 1982).

An alternate interpretation of the sometimes weak particle effects on slurry atomization, that is based on fluid continuum properties, is as follows.

First, we assume that the slurry particles are elastic. Also, we assume that bulk transfers of momentum by viscous effects, on the scale of the atomizing eddies, are not strongly affected by the solid particles, which might not be true when the solids volume

fraction is large and the drops are not small compared to the solid particles.

Suppose that most of the spray liquid is in drops that contain a large number of solid particles. This indicates that during atomization the particle motion relative to the surrounding bulk liquid creates flow disturbances in the liquid that have small scale relative to the eddies that deform the slurry-gas interface. It follows that such particle-scale disturbances are strongly inhibited by viscous forces, and do not interact directly with the atomizing eddies. (The basic flow is unstable. This leads to eddies that deform the liquid-gas interface. Smaller-scale eddies would be even more unstable, but do not appear due to strong damping by viscous forces. Smaller-scale particle induced disturbances are also strongly damped.) Thus, little energy is imparted to such particle induced disturbances. Further, if the particle material density is close to the liquid density, the forces that accelerate the surrounding bulk liquid also accelerate the particles at nearly the same rate. Thus, the particles develop little relative motion even if the liquid is inviscid. Examples are a slurry in a gravity field, or under centrifugal acceleration as in a centrifuge; if the particle material density is the same as the liquid, the particles remain suspended (develop no relative motion).

Suppose, on the other hand, that most of the spray liquid is in drops that contain no solid particles. This occurs at higher pressure conditions, when the atomizing eddies are smaller than the suspended particles. The result is that many of the drops formed contain only the liquid originally surrounding the particles. Thus, the atomization is nearly optimum in that the surrounding liquid is simply stripped from the particles by interaction with the gas (Gaag, 1984).

In summary, when the observed slurry spray drops tend to have either no solid particles or a very large number of solid particles, it follows that the solid particles do not interact strongly with the atomizing

eddies, and that atomization performance is very similar to that of the liquid carrier in the absence of solid particles. It appears that the solid particles should substantially affect atomization performance only when three conditions are satisfied for drops containing most of the slurry volume: first, the solid particle size is not small compared to the slurry drop size; secondly, most of the slurry drops contain a small number of solid particles; and thirdly, the solid particle material density is substantially different from the liquid carrier.

### 3. ATOMIZATION IN OPPOSED SWIRL NOZZLES

In Section 2, we concentrated on general fluid mechanisms involved in atomization. However, this does not provide detail on just how these mechanisms operate in a given nozzle. For this, we need more detailed observations and fluid models. However, useful partial theories can be derived from known fluid behavior. This assumes that fluid properties are at least qualitatively maintained in the small space and time scales typically involved in atomization.

We now apply known fluid behavior to derive a partial theory on atomization dynamics in an opposed swirl nozzle (Dietrich, 1982, 1985; Simmons, 1984; Gaag, 1984). An opposed swirl nozzle is an internal mix nozzle into which the fluids to be mixed or atomized are injected with opposed swirl (angular) velocity components.

A simple version of this nozzle has a basically axisymmetric cavity with one end closed (Figure 1). The other end has a central opening through an orifice piece. The cavity is divided into two chambers by an axisymmetric throat piece with central opening. Fluid A is injected into chamber A, the chamber farthest from the orifice. Fluid B is injected into chamber B. Fluid A is directed through one or more side ports with an angular velocity component (also called swirl). Fluid B is directed through

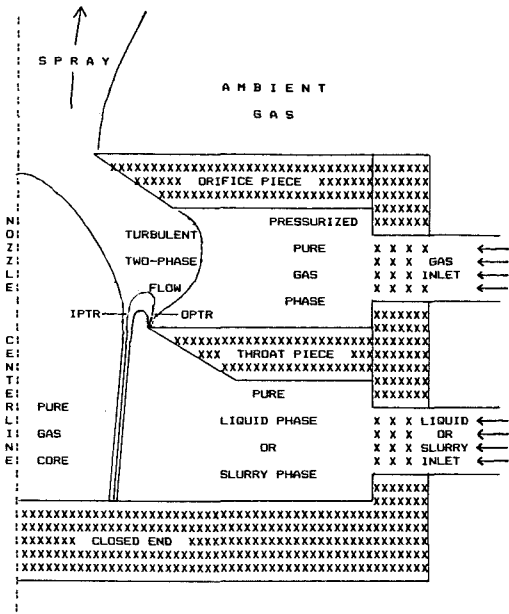


**FIGURE 1.** Plane cut through centerline of idealized balanced swirl nozzle with schematic time-averaged fluid density contours. The contours are drawn only to illustrate qualitative flow features consistent with partial theory in text.

one or more side ports with swirl opposite to that of fluid A. Ideally, the angular momentum inflow rate into chamber A approximately balances its inflow into chamber B.

When fluid A is a liquid and fluid B is a gas, some likely aspects of the dynamics of this nozzle are as follows. We assume fluid accelerations are large compared to gravity.

Under high Reynolds number operation, a well-developed vortex fills chamber A. The swirl distribution is described approximately by angular momentum conservation. Thus, swirl velocity increases toward the centerline. However, the liquid does not reach the centerline. This would require extremely high pressure to approximately conserve angular momentum. Instead, the liquid penetrates only to a radius just inside the throat opening, leaving a gas core around the centerline. The liquid then accelerates axially, forming a nearly axisymmetric swirling thin

cylindrical sheet as it passes through the throat and enters chamber B (Figure 1).

The pressure force necessary for this axial acceleration through the throat opening implies that the gas core diameter is smaller near the closed end of chamber A than near the throat. The nearly uniform pressure at the interface between the swirling liquid and the gas core, together with the inward force needed to keep the interface from moving outward, then implies higher pressure in the liquid vortex near the closed end of chamber A than at the same radius near the throat. The liquid speed at the gas core interface is nearly constant, consistent with a Bernoulli relation at such nearly constant pressure surface. However, the ratio of axial to swirl velocity magnitude varies greatly, increasing toward the throat.

The swirling thin sheet entering chamber B immediately encounters counter-swirling gas at its outer surface, as the gas flow in chamber B also includes a well-developed vortex outside the throat opening. In the basic (time averaged) flow, there is a transition region between the region always occupied by liquid and the region always occupied by gas. We call this the phase transition region or PTR. There is an inner IPTR between the liquid sheet entering chamber B and the centerline, and an outer OPTR between liquid sheet and the chamber B gas inlets (Figure 1).

The averaged fluid density in the OPTR varies between the bulk liquid and bulk gas density. Two mechanisms dictate that flow distribution in the OPTR is very unstable. The basic swirl and density distribution provides an instability mechanism that is analogous to having dense fluid above less dense fluid in a gravity field, as in Rayleigh–Taylor instability. The basic swirl distribution provides a second instability mechanism, analogous to the classical centrifugal Taylor instability in swirling flows (Monin and Yaglom, 1971). These two mechanisms could lead to a bimodal drop size distribution. A similar double instability mechanism causes

a “spectral gap” in atmospheric flow eddy sizes (Dietrich, 1977; Hogstrom and Hogstrom, 1975).

The fluid instabilities in the OPTR imply rapid growth of turbulent eddy energy in the fluid entering the OPTR. The turbulent eddies deform the outer (farthest from the chamber centerline) liquid sheet surface and shear liquid elements away, thereby widening the OPTR. Thus, the OPTR width (transverse to the basic flow) increases along the basic flow trajectories. Thus, turbulent mixing entrains liquid and gas into the OPTR, and reduces the basic velocity and density gradients downstream from the throat. The remaining bulk liquid stream inside (closer to the chamber centerline) the OPTR retains its original swirl angular momentum, as does the gas outside the OPTR. Such configuration is still unstable, but the turbulent eddies that grow in the widened OPTR have larger scales in order to communicate across the OPTR. Indeed, such larger scale eddies can grow very rapidly, as the effective Reynolds number of the OPTR is very large, especially if one ignores interaction of such larger-scale eddies with the smaller ones that widened the OPTR upstream.

Thus, one expects that small drops should form in the region just downstream from the throat opening, with larger drops forming further downstream in a wider OPTR. This is one possible mechanism for the large range of drop sizes that are observed in most nozzles. The maximum drop sizes should be produced by eddies whose scale is comparable to the remaining bulk liquid sheet thickness, after the outer part of the sheet has been eroded and atomized, and the OPTR width is comparable to the remaining sheet thickness. This is consistent with the observation that sheet thickness is well correlated to drop size (Simmons, 1979).

This theory was briefly described in (Dietrich, 1985). Since then, it has been supported by observations of similar phenomena involving fluid instabilities in dif-

ferent geometries. In Rayleigh–Taylor instability experiments (see Appendix B), eddy sizes grow as the mixed region resulting from the eddies widens with time. In the breakup of an axisymmetric jet, eddy sizes also grow as the mixed region grows downstream from a nozzle orifice (Cohen and Wyganski, 1987). Results from an interesting study (Knoll and Sojka, 1987; see Appendix C) further support this theory.

In the classical Taylor–Couette experiments, centrifugal instabilities tend to produce quasi-axisymmetric vortices, with large angular modulation scale compared to the vortex cross-sections (Barcilon et al., 1979). Thus, the vortices are quasi-toroidal. Such quasi-toroidal eddies probably also occur in the above discussed opposed swirl nozzle, especially if the eddy capillary number  $\nu \Delta U / \sigma$ , where  $\Delta U$  is the basic flow velocity difference on the scale of the eddies, is large. However, the ratio of angular length scale to toroidal cross-section diameter of the most unstable eddies should increase with increasing capillary number. This key length ratio can be called the “capillarity,” and is usually greater than 1. As the unstable eddies move downstream into a widened OPTR, their capillarity should decrease (due to decreased basic flow velocity change on the scale of the eddies). Thus, the ligaments produced by the originally quasi-toroidal eddies “pull together” and separate from the remaining bulk liquid.

The situation is different for the eddies that develop in the widened OPTR downstream. Their toroidal cross-section is wider than the upstream eddies, in order to communicate across the widened OPTR. Also, the eddy viscosity effect of the smaller-scale eddies that formed upstream should increase the effective capillarity of the larger-scale most unstable eddies in the widened OPTR. Thus, both the toroidal cross-section diameter and the angular length scale of the most unstable eddies should increase as one moves downstream into the widened OPTR. Similar interaction between small-

scale and large-scale structures has been noted in Taylor–Couette experiments (Barcilon et al., 1979). The upstream eddies might be involved in observed satellite drop formation.

These mechanisms are also applicable to the atomization of liquid slurries.

The important Taylor instability occurs at relatively low Reynolds numbers and is common in nature. Its effects occur whenever the basic flow has significant curvature, as can be induced by curved boundaries. Its occurrence at low Reynolds number increases its effects in nature and, in view of the computational cell Reynolds number limit (Roache, 1982), reduces resolution and computation required to realistically address phenomena involving it. Mathematical models of mixing and atomization processes are discussed in Dietrich (1987).

Taylor instability can help control turbulence. In axisymmetric geometries, this is achieved by forcing a basic flow swirl distribution that is unstable/overstable in regions where it is desired to increase/decrease turbulence. Not surprisingly, axisymmetric Taylor–Couette experiments are among “the best known problems in the whole field of fluid mechanics” (Barcilon et al., 1979), and when the Taylor instability mechanism is used in the opposed swirl nozzles discussed above, very efficient atomization can occur. Indeed, according to data given in Simmons (1984) and Gaag (1984), the opposed swirl nozzle produces drops with Sauter mean diameter about 5/12 the size produced by modern gas turbine airblast nozzles under similar operating conditions. Since the energy required to atomize a liquid is quadratically related to the drop size (see Appendix A), this indicates almost a factor of 6 energy savings in producing given required drop size.

Although the opposed swirl nozzle is generally a very efficient nozzle and also has other desirable properties (Dietrich, 1982, 1985; Simmons, 1984; Gaag, 1984), it ideally should be operated in such a manner that

the net angular momentum inflow rate into the nozzle is near zero, so that the opposed swirls nearly cancel during the mixing process inside the nozzle. It can be designed to operate in such a manner for any desired mass flow ratio. Details on judicious design and operation of this nozzle are given in Dietrich (1990).

#### 4. SUMMARY AND CONCLUDING REMARKS

Observations and general fluid mechanisms have led to a partial theory of mixing and atomization processes, including some detailed theories based on these mechanisms in balanced swirl nozzles. According to the theory, quasi-toroidal (axisymmetric) elongated eddies that result from Taylor (centrifugal) and Rayleigh–Taylor instabilities play a major role in determining drop size, and surface tension effects are secondary under normal high-velocity operating conditions. Nonlinear mixing by the early (upstream) atomizing eddies that develop near the concentrated gradient zones where the bulk liquid and air initially interact is probably a primary cause of larger-scale eddies developing downstream and leading to larger drop sizes.

---

I would like to warmly acknowledge my father, Dr. Verne Dietrich, and Mr. Harold Simmons for insight derived from many stimulating discussions.

---

#### APPENDIX A

##### Pressurization Effects on Drop Size

As noted in Dietrich (1982), the length scale of eddies resulting from fluid dynamic instabilities determines drop diameters. A scaling estimate of drop diameter was also derived in Dietrich (1982). We summarize the derivation here.

In order for any basic (time averaged) flow to be fluid dynamically unstable, the eddy perturbation energy source must be larger than the energy sink. In the momentum conservation equations, the inertia

terms are the only possible eddy energy source; surface tension and viscous terms dissipate kinetic energy (in the process of atomization, surface area and surface energy increase). Here, and in the ensuing discussion, we ignore gravity effects. The forces (per unit volume) in the momentum conservation equations can then be scaled as follows:

$$\text{inertial force} \sim \rho U^2/L$$

$$\text{viscous force} \sim \rho U/L^2$$

$$\text{surface tension force} \sim \sigma/L^2,$$

where  $U$  is a basic flow velocity,  $L$  is the eddy length scale,  $\nu$  is the viscosity coefficient, and  $\sigma$  is the surface tension coefficient.

The three proportionality factors depend on the injection configuration and nozzle shape. Thus, in order to have a balance among eddy energy sources and sinks,

$$\rho UL / \{ \nu [1 + (W_c/R_c)\sigma/(\nu U)] \} = R_c, \quad (1)$$

where  $W_c$  and  $R_c$  depend on the injection configuration and nozzle shape, and  $\nu U/\sigma$  is a capillary number.  $R_c$  can be interpreted as a critical Reynolds number when the capillary number is large.  $W_c$  can be interpreted as a critical Weber number when the capillary number is small.

Eq. (1) can be written

$$L = R_c [1 + W_c \sigma / (\nu U)] / \rho U \\ = K_1 / U + K_2 / U^2. \quad (2)$$

For a given nozzle, the parameters  $R_c$ ,  $W_c$ ,  $K_1$ , and  $K_2$  depend on the fluid density ratio, viscosity ratio, and mass flow ratio. If one assumes  $U \sim (\Delta p)^{0.5}$ , as in a Bernoulli relation, Eq. (2) can be written

$$L = K_1 / (\Delta p)^{0.5} + K_2 / (\Delta p). \quad (3)$$

The first term dominates at sufficiently large pressure drops. This means that viscous forces are more important than surface tension forces in determining drop size when the pressure drop is sufficiently large. Data correlation studies (Jasuja, 1978; Dietrich,

1982; Elkolb and Abdalla, 1982; Jones, 1982) show that the first term usually dominates under typical nozzle operating conditions.

## APPENDIX B

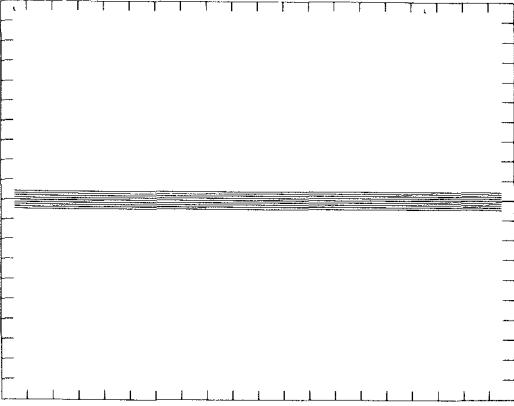
### Rayleigh–Taylor Instability Observations

Rayleigh–Taylor experiments have a flow evolution like the sequence of linear and nonlinear dynamic processes proposed in Dietrich (1985) as a primary cause of the wide range of drop sizes coming from spray nozzles, and discussed in more detail in Section 3 of this paper. The potential importance of this dynamic sequence in nozzles was further supported in Cohen and Wyganski (1987). Since these experiments are quasi-two-dimensional and are particularly easy to model on a computer, we use model results to illustrate the sequence discussed in Section 3. The calculations take less than 5 min on a Microvax 2 computer.

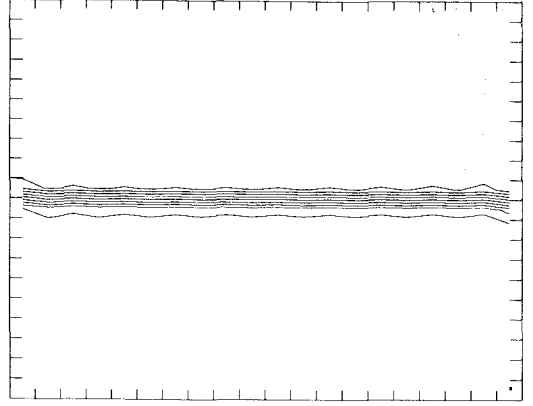
In the computer simulation, a nearly stationary, uniform density, cool gas (298°K) initially overlies a relatively warm gas (328°K) at the same initial pressure and mean molecular weight (therefore, lower density). The interface between the cool and warm gas is initially horizontal (Figure 2a), but a small semirandom velocity perturbation is assumed throughout the gas. The initial perturbation and ensuing flow are assumed independent of one horizontal coordinate. The grid interval is 1 cm, and there are 20 zones in each direction. Constant momentum and heat diffusivities of 0.2 cm<sup>2</sup>/s are assumed.

Figure 2 shows the sequence of ensuing flows. Since the flow Mach number remains very small, the pressure remains relatively constant and temperature is inversely related to density. Except for the boundary effects, the sequence is qualitatively similar to the sheet breakup theory proposed in Section 3 (considering the time sequence of the mean temperature contour to be analogous to a time sequence of local environ-

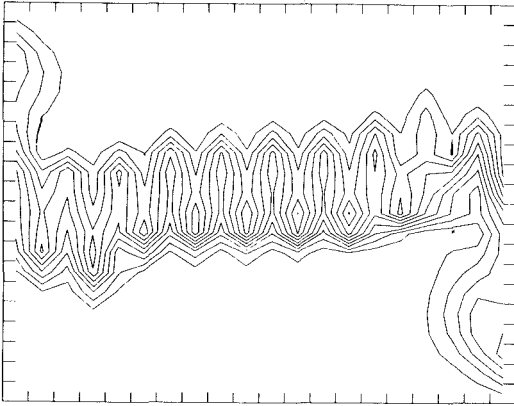




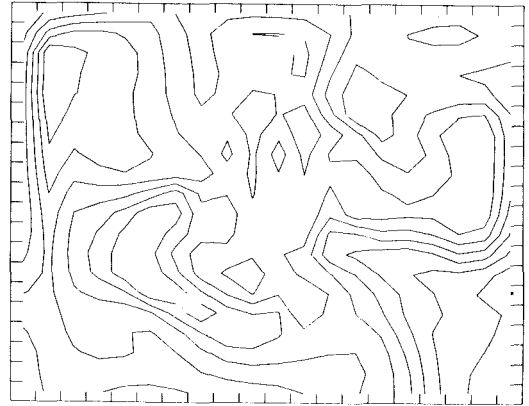
(a)



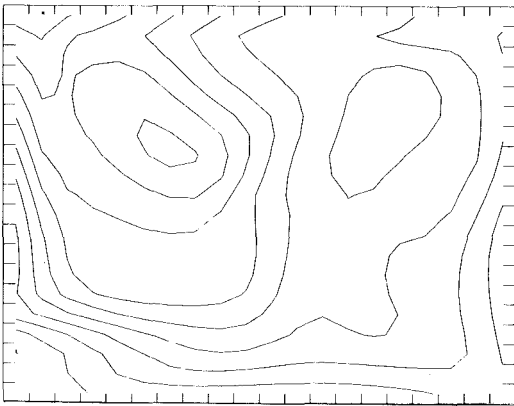
(b)



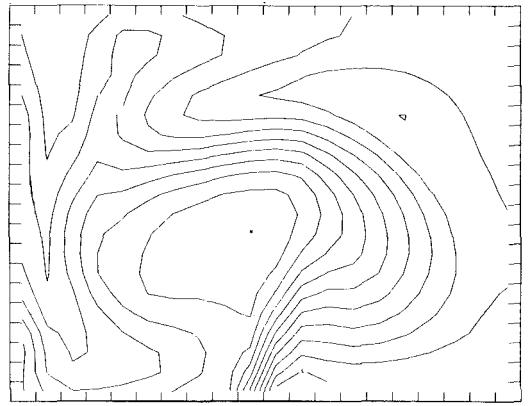
(c)



(d)



(e)



(f)

ments “seen” by individual fluid material elements inside the nozzle).

Note the early development of a characteristic scale oscillatory deformation of the interface between the cool and warm gas (Figure 2*b*). This reflects a scale selection involving Rayleigh–Taylor instability with a viscous cutoff. The deformation grows in amplitude and mixes the two fluids. As the mixed region widens (Figure 2*c–f*), larger eddy scales dominate, until the dominant eddies have comparable scale to the experimental dimensions.

An early nonlinear effect is the development of a double structure in the vertical (Figure 2*c*) when the vertical scale of the interface deformation becomes comparable to the horizontal scale of the growing eddies.

This can be explained as a result of mixing by the early eddies.

The early eddies’ energy is concentrated near the original density discontinuity. Thus, they mix only in this narrow region. The result is that the vertical profile of the horizontally averaged density in the mixed layer

approaches the mean of the two material densities, with jumps to the original high and low material density at the top and bottom of the mixed layer, respectively.

The new mean (horizontally averaged) density profile environment favors eddies whose energy is concentrated at the top and bottom of the mixed layer, resulting in a double structure. Interestingly, a double structure is also shown in schematic pictures on liquid sheet disintegration (Dombrowski and Johns, 1963).

The double structure eddies increase the density at the top of the original mixed-layer region, and decrease it at the bottom. The resulting finite-depth unstable mixed layer favors the development of larger horizontal scale eddies. The sequence continues (Figure 2*d–f*), and larger and larger horizontal scales are favored until the entire region is mixed (Figure 2*f*). Note that the mixing leads to significantly reduced temperature contrast. In the absence of mixing, it would have taken much longer to reduce the temperature contrast by conduction. Later in the calculation (not shown), the temperature again becomes nearly horizontally stratified, but with reduced contrast, diffused gradient, and the cooler gas under the warmer gas.

If the horizontal scale of the early most unstable eddies were equal to or larger than the depth of the experiment, the range of eddy scales that develop would be reduced. Three possible ways to do this are as follows. The first is to make the original density profile continuous, such as a linear profile from top to bottom. A second way, which would retain the density discontinuity at middepth, would be to limit the depth of the experiment to a value less than or equal to the horizontal scale of the most favored eddies that occur in much deeper experiments. A third way is to favor the action of eddies comparable to the experimental depth by putting them in at large amplitude initially, which can be done more easily numerically than in the laboratory.

---

**FIGURE 2.** Time sequence showing linear and nonlinear dynamics of Rayleigh–Taylor instability in vertical slab: temperature (degrees Kelvin) at various model times:

- (a) time step 50, time = 0.27 s  
(min = 298, max = 328, Re = 12.5)
- (b) time step 100, time = 0.68 s  
(min = 298, max = 328, Re = 46.8)
- (c) time step 200, time = 2.11 s  
(min = 298, max = 328, Re = 94.8)
- (d) time step 400, time = 4.16 s  
(min = 300, max = 327, Re = 96.0)
- (e) time step 600, time = 6.16 s  
(min = 306, max = 318, Re = 95.8)
- (f) time step 800, time = 9.64 s  
(min = 309, max = 316, Re = 91.6),

where the Reynolds number Re is based on the maximum velocity and the 20-cm domain size. The crude resolution used is sufficient to illustrate the primary mechanisms observed in the Rayleigh–Taylor experiments.

The latter two methods might both be useful in reducing the range of drop sizes from nozzles by appropriate nozzle design and operating conditions. This could be done by controlling the liquid sheet thickness appropriately and/or by adding controlled finite amplitude perturbations of appropriate frequency to the bulk liquid flow upstream.

## APPENDIX C

### Variable Air-Gap Studies

Results from a very interesting study of an air-assisted atomizer were reported at ILASS-87 (Knoll and Sojka, 1987). In this study, the air pressure (and velocity) are held fixed while varying the air gap and liquid mass flow in such a manner that the air-to-liquid mass flow is constant. It was found that increasing air gap results in larger drop sizes under these conditions. One possible explanation, given in Knoll and Sojka (1987), is that some of the air in the widened air stream, being well separated from the liquid, loses energy in mixing with air outside the nozzle rather than in mixing and atomizing the liquid. Another possible explanation, according to the theory in Section 3, is that the mixed region gets much wider before the air energy is used up, resulting in larger atomizing eddies. Probably, both mechanisms contribute to the larger drops observed. This well-designed and significant study shows the importance of nozzle geometry in atomization performance—the ratio of the atomizing air power to the bulk liquid mass flow rate was held constant for different nozzle designs (air gap width), yet smaller air gaps consistently led to smaller drop sizes, thereby conclusively demonstrating that the small air-gap design was superior in terms of atomizing efficiency.

## NOMENCLATURE

IPTR inner phase transition region  
 $K_1, K_2$  empirical constants

$L$  typical eddy length scale  
 OPTR outer phase transition region  
 $\Delta p$  external pressure difference  
 $R_c$  critical Reynolds number  
 $U$  typical flow velocity  
 $\Delta U$  typical velocity difference on the scale of the eddies  
 $\rho$  typical density  
 $W_c$  critical Weber number  
 $\sigma$  surface tension coefficient  
 $\nu$  momentum diffusion coefficient (viscosity)

## REFERENCES

- Barcilon, A., Brindley, J., Lessen, M., and Mobbs, F. R. (1979). *J. Fluid Mech.* 94:453–463.
- Cohen, J., and Wagnanski, I. (1987). *J. Fluid Mech.* 176:191–219.
- Dietrich, D. E. (1977). *Atmosphere* 15:1–18.
- Dietrich, D. E. (1982). In *Proceedings of Second International Conference on Liquid Atomization and Spray Systems*. Madison, WI, pp. 161–168.
- Dietrich, D. E. (1985). In *Encyclopedia of Fluid Mechanics* (N. P. Chermisinoff, ed.), Syntax International, Singapore, vol. 3, pp. 365–370.
- Dietrich, D. E. (1987). *Atomization Spray Technol.*, 3:291–308.
- Dietrich, D. E. (1990). *Aerosol Sci. Technol.* This issue.
- Dombrowski, N., and Johns, W. R. (1963). *Chem. Eng. Sci.* 18:203–214.
- Elkoth, M. M., and Abdalla, M. A. (1982). In *Proceedings Second International Conference on Liquid Atomization and Spray Systems*. Madison, WI, pp. 237–244.
- Gaag, J. (1984). *Practical Application of External Mix Slurry Atomizers*, presented at Fourth Annual Coal Liquid-Mixtures Workshop, October 9–11, 1984. Parker Hannifin Corp., Gas Turbine Fuel Systems Division, Cleveland, OH.
- Hogstrom, A. S., and Hogstrom, U. (1975). *J. Atmos. Sci.* 32:340–350.
- Jasuja, A. K. (1978). *Atomization of Crude and Residual Fuel Oils*, ASME paper 78-gt-83.
- Jones, A. R. (1982). In *Proceedings of Second International Conference on Liquid Atomization and Spray Systems*. Madison, WI, pp. 181–185.
- Knoll, K. E., and Sojka, P. E. (1987). Talk given at ILASS Americas-87, Madison, WI, June 8–11.

- Monin and Yaglom (1971). *Statistical Fluid Mechanics*. MIT Press, Cambridge, MA, vol. 1, pp. 96–106.
- Roache, P. J. (1982). *Computational Fluid Dynamics*. Hermosa Publishers, Albuquerque, NM.
- Simmons, H. C. (1979). *The Atomization of Liquids*, Report #7901/2. Parker Hannifin Corp., Gas Turbine Fuel Systems Division, Cleveland, OH.
- Simmons, H. C. (1984). *The Atomization of Slurries*, Report BTA 141, presented at Sixth International Symposium on Coal Slurry Combustion and Technology, June 25–27, 1984. Parker Hannifin Corp., Gas Turbine Fuel Systems Division, Cleveland, OH.

Received July 20, 1987; accepted December 16, 1988.